



ELSEVIER

Contents lists available at ScienceDirect

Cancer Letters

journal homepage: www.elsevier.com/locate/canlet

Original Articles

Glioma cell dispersion is driven by $\alpha 5$ integrin-mediated cell–matrix and cell–cell interactions

Anne-Florence Blandin ^a, Fanny Noulet ^a, Guillaume Renner ^a, Marie-Cécile Mercier ^a, Laurence Choulier ^a, Romain Vauchelles ^a, Philippe Ronde ^a, Franck Carreiras ^{a,b}, Nelly Etienne-Selloum ^a, Gyorgy Vereb ^{a,c}, Isabelle Lelong-Rebel ^a, Sophie Martin ^a, Monique Dontenwill ^a, Maxime Lehmann ^{a,*}

^a *Integrins and Cancer, Faculté de Pharmacie, UMR7213 CNRS, LBP, Tumoral Signaling and Therapeutic Targets Department, Université de Strasbourg, Illkirch, France*

^b *Equipe de Recherche sur les Relations Matrice Extracellulaire Cellules, ERRMECe (EA 1391), Institut des Matériaux, Université de Cergy-Pontoise, France*

^c *Department of Biophysics and Cell Biology, Faculty of Medicine, University of Debrecen, Hungary*

ARTICLE INFO

Article history:

Received 26 January 2016

Received in revised form 1 April 2016

Accepted 4 April 2016

Keywords:

Glioblastoma

Integrin

Fibronectin

Focal adhesion kinase

Migration

ABSTRACT

Glioblastoma multiform (GBM) is the most common and most aggressive primary brain tumor. The fibronectin receptor, $\alpha 5$ integrin is a pertinent novel therapeutic target. Despite numerous data showing that $\alpha 5$ integrin support tumor cell migration and invasion, it has been reported that $\alpha 5$ integrin can also limit cell dispersion by increasing cell–cell interaction. In this study, we showed that $\alpha 5$ integrin was involved in cell–cell interaction and gliomasphere formation. $\alpha 5$ -mediated cell–cell cohesion limited cell dispersion from spheroids in fibronectin-poor microenvironment. However, in fibronectin-rich microenvironment, $\alpha 5$ integrin promoted cell dispersion. Ligand-occupied $\alpha 5$ integrin and fibronectin were distributed in fibril-like pattern at cell–cell junction of evading cells, forming cell–cell fibrillar adhesions. Activated focal adhesion kinase was not present in these adhesions but was progressively relocalized with $\alpha 5$ integrin as cell migrates away from the spheroids. $\alpha 5$ integrin function in GBM appears to be more complex than previously suspected. As GBM overexpressed fibronectin, it is most likely that *in vivo*, $\alpha 5$ -mediated dissemination from the tumor mass overrides $\alpha 5$ -mediated tumor cell cohesion. In this respect, $\alpha 5$ -integrin antagonists may be useful to limit GBM invasion in brain parenchyma.

© 2016 Published by Elsevier Ireland Ltd.

Introduction

Glioblastoma multiform (GBM, grade IV astrocytoma) is the most frequent and most aggressive brain cancer. Despite surgical resection, radiotherapy and concomitant chemotherapy, median survival for a patient with high grade glioma does not exceed 15 months. GBM is characterized by a diffuse infiltration of the brain tissue by tumor cells. This highly invasive phenotype prevents complete surgical resection, limits the efficiency of radiotherapy and is a critical prognostic factor for primary brain tumors. The establishment of efficient therapies requires a better understanding of the infiltrative behavior of glioma cells and the development of new strategies targeting cell invasion [1,2]. *In situ*, glioma cells individually infiltrate the brain tissue either by migrating along the blood vessels or by invading the parenchymal tissue [3,4]. Invasion is modulated by regional expression of extracellular matrix (ECM) molecules [5,6]. Some ECM proteins are overexpressed in human brain tumors

and their upregulation correlates with disease progression and worse prognosis. Comparison of gene expression in invasive GBM versus non-invasive pilocytic astrocytoma using suppressive hybridization identified fibronectin (FN) as one of the most overexpressed gene in GBM [7]. FN accumulates around neovasculature [8,9] and into tumor ECM as dense linear strands of assembled FN surrounding cancer cells [10–13]. FN supports tumor growth [14] and is unequivocally capable of mediating glioma cell motility and promoting invasion [11,13,15].

As primary receptors involved in cell–matrix adhesion, integrins bidirectionally link the ECM with the intracellular signaling network. They profoundly impact on tumor cell proliferation, survival and invasion, and trigger resistance to radio- and chemo-therapy [16]. In human brain, the FN receptor, $\alpha 5 \beta 1$ integrin, is expressed at significantly higher level in GBM than in adjacent normal tissue [17]. We [18,19] and others [20–22] recently confirmed these data in larger cohorts of patients and showed that a high expression of $\alpha 5 \beta 1$ integrin is associated with a worse prognosis. Preclinical data support the ability of $\alpha 5 \beta 1$ integrin antagonists to disrupt integrin signaling pathways leading to inhibition of angiogenesis and/or tumor growth but also to sensitization toward therapies [23]. Depletion

* Corresponding author. Tel.: +33 368854267; fax: +33 368854313.

E-mail address: Maxime.lehmann@unistra.fr (M. Lehmann).

of $\alpha 5$ integrin increased p53 activity and sensitized cells to chemotherapeutic agents [19,24]. Moreover $\alpha 5\beta 1$ integrin antagonists facilitated chemotherapy-induced apoptosis in human glioma cells [24,25]. Collectively, these data establish $\alpha 5\beta 1$ integrin as a promising target in GBM. $\alpha 5$ integrin mediates fibronectin assembly, an essential process that regulates cell morphology, growth and motility [26]. On 2D cell culture, fibrillogenesis is initiated by $\alpha 5$ integrin in cell-substratum adhesion sites called fibrillar adhesion (FBs). FBs are functionally and molecularly distinct from the classical focal adhesion (FAs) as they did not contain activated FAK (focal adhesion kinase) or other FAs proteins such as paxillin or vinculin [27,28]. Drug-mediated inhibition of FN fibrillogenesis sensitizes glioma cells to chemotherapy *in vitro* and *in vivo* [12]. Fibrillar FN/ $\alpha 5$ axis may thus play a pivotal role in glioma resistance to therapy and invasion.

Using single cell tracking assays, we showed that expression of $\alpha 5$ integrin in U87MG cells increased cell migration speed, which could be inhibited by the use of specific non-peptidic antagonists of $\alpha 5\beta 1$ integrin [29,30]. However, other reports showed that $\alpha 5\beta 1$ and fibrillary FN can promote cell/cell cohesion in various tissue [13,31–33] and may impair glioma cell dispersion [32]. This observation point out a potential anti-invasive role for $\alpha 5\beta 1$ and cell-mediated FN assembly. This may raise an important issue concerning the development of anti-invasive therapeutic strategies that target $\alpha 5\beta 1$ integrin.

In the present work, we showed that $\alpha 5$ -mediated cell-cell interaction can counteract cell dissemination only if fibronectin is absent from tumor cell microenvironment. We observed that in cells collectively emerging from the spheroid, $\alpha 5$ integrin delineated plasma membrane in a fibrillar-like pattern and is associated with a dense FN fibril network. Importantly, activated FAK (pFAK-tyr397) was not recruited by $\alpha 5$ integrin in these cell-cell fibrillar adhesions. As cells moved away from the spheroids, $\alpha 5$ became strictly engaged in cell-substratum adhesion sites, where it progressively recruited pFAK-tyr397. In conclusion, our data indicate that in GBM $\alpha 5$ integrin may have different function and that glioma cell invasion is regulated by the balance between $\alpha 5$ -mediated cell-cell and cell-substratum interaction.

Material and methods

Reagents

Function blocking antibodies directed against $\alpha 5$ integrin, clone IIA1 was from BD Biosciences and against αv integrin, clone 69.6.5 was produced and purified as previously described [34]. Following antibodies were used for confocal microscopy. Conformation dependent LIBS anti- $\alpha 5$ antibody clone SNAKA-51 was from Millipore. Phycoerythrin-conjugated anti- $\alpha 5$ antibody (clone SAM-1) was from BioLegend. Anti- $\beta 1$ antibody clone TS2/16 was produced from the hybridoma cell line TS2/16.2.1 (HB-243, ATCC) and purified on protein-G-sepharose column (Pierce). Anti- αv antibody, clone PLW7, was from Santa Cruz Biotechnology, anti-fibronectin antibody, clone 10, was from BD Biosciences, anti-pFAK-tyr397, clone 141-9 from Life Technologies. Fluorescently labeled secondary antibodies were purchased from Invitrogen (Alexa Fluor –488; –546; –647). Dapi was purchased from Santa Cruz Biotechnology. Human fibronectin stabilized solution was purified as described in Reference 35. Cell culture medium and reagents were from Lonza. All other reagents were of molecular biology quality.

Cell culture

The human glioblastoma cell line U87MG was obtained from ATCC. U87MG cells were maintained in Eagle's minimum essential medium (EMEM) supplemented with 10% fetal bovine serum (FBS), 1% L-glutamine, 1% sodium pyruvate and 1% non-essential amino-acid, in a 37 °C humidified incubator with 5% CO₂. U87MG cells were transfected with plasmid encoding $\alpha 5$ cDNA or specific shRNA targeting $\alpha 5$ mRNA as described [19], except that after selection with antibiotics, stably transfected cells were mass-selected by two steps of cell sorting (FACSAria™ II, BD Bioscience) using PE-conjugated SAM-1 antibody. We selected cells expressing various amount of $\alpha 5$ integrin. Cell surface expression of $\beta 1$ and αv subunits were controlled by flow cytometry analysis (10,000 cells analyzed for each condition) using TS2/16 and 69-6-5 monoclonal antibodies respectively. $\alpha 5$ and $\beta 1$ integrin expression levels were further analyzed by immunoblot using IIA1 and TS2/16 monoclonal antibodies as described [19]. In the present study we used U87 cells transfected with pcDNA3.1 $\alpha 5$

as high $\alpha 5$ expressing cells (U87 $\alpha 5+$) and U87 cells expressing $\alpha 5$ -shRNA as low $\alpha 5$ expressing (U87 $\alpha 5-$). LN229 and LN443 cells were cultured as described in Reference 24. LN229 cells were transfected as described for U87 cells. LN229 clonal populations were obtained by limited dilution and clones expressing various amount of $\alpha 5$ integrin were selected.

Proliferation assay

Cells were plated (1000 cells/well) onto a 96-well plate in EMEM supplemented with 10% FBS. At indicated times, cell viability was determined using a tetrazolium compound [3-(4,5-dimethyl-2-yl)-5-(3-carboxymethoxyphenyl)-2-(4-sulfophenyl)-2H-tetrazolium, inner salt (MTS assay – CellTiter 96 Aqueous One Solution Cell proliferation assay from Promega).

Spheroid formation

Six grams of methylcellulose was dissolved in 250 mL of EMEM and heated at 60 °C for 1 h. The solution was then kept at 4 °C under agitation for 18 hours. The solution was cleared by centrifugation (5000 g, 2 h). Single cell suspension was generated from trypsinized monolayers and diluted at the desired cell density. Cell suspension was mixed in EMEM/10%FBS containing 20% of methylcellulose. All the spheroids were made with 2000 cells. Cell spheroids were formed by hanging drop methods (25 μ L, 2000 cells per sphere) on a U-bottom 96 well plate (Greiner Cellstar U-bottom culture plate) (100 μ L, 2000 cells).

Spheroid organization

Spherical organization of 20 spheroids/condition was followed regularly from 0 to 48 hours on phase-contrast images (EVOS xl Core, 20 \times magnification). Circularity measurements (roundness) were measured using shape descriptors of ImageJ software [36]. When indicated function blocking anti-integrin antibodies (anti- $\alpha 5$, clone IIA1; anti- αv , clone 69.6.5) were added at 10 μ g/mL in the cell suspension.

Spheroid migration assays

Plastic dishes were coated with poly-L-lysine (10 μ g/mL) or fibronectin (indicated concentration) in PBS solution for 2 h at 37 °C. Two-day old spheroids were allowed to adhere to 24-well plates in complete medium (EMEM, 10% FBS). Eighteen hours later, cells were fixed with paraformaldehyde 3.7% (Electron Microscopy Sciences) and stained with DAPI. Phase-contrast images (EVOS xl Core, 5 \times magnification) were acquired. Cell number was quantified with a home-made macro using ImageJ software.

Confocal microscopy and image analysis

Coverslips were coated with fibronectin (10 μ g/mL in PBS). Two-day old spheroids were seeded in complete medium for 18 hours. Cells were then fixed in 3.7% paraformaldehyde, and permeabilized with 0.1% Triton-X100. After a 1 hour blocking step using TBS-BSA 3% solution, cells were incubated with primary antibodies O/N at 4 °C (2 μ g/mL each in TBS-BSA 3%). Cells were incubated with appropriate secondary antibodies (1 μ g/mL in TBS-BSA 3%) and DAPI for 1 hour. Spheroids were mounted on microscope slides using Permafluor Aqueous Mounting Medium (Fisher). Images were acquired using a confocal microscope (LEICA TCS SPE II, 60 \times magnification oil-immersion). Feret's diameter used as adhesion size criteria were quantified using an ImageJ plugin developed in the lab. Pearson correlation coefficient was calculated using JACoP plugin ImageJ software [37]. Suspended spheroids were fixed with 3.7% paraformaldehyde, and permeabilized with 0.1% Triton-X100 for 5 min. Saturation and immunolabeling were performed on U-bottom 96 well plates.

Immunostaining on patient-derived xenograft

A patient-derived integrin $\alpha 5$ expressing glioblastoma xenograft was selected for *in vivo* analysis as described in Reference 19. Briefly, formalin-fixed paraffin-embedded xenograft was prepared as previously described [19] and 4 μ m sections were deparaffinized, rehydrated and subjected to unmask the antigen protocol using Dako retrieval solution pH9. Next, blocking buffer (5% Goat serum, 0.1% Tween-20, PBS) was applied for 1 hour at room temperature. Integrin $\alpha 5$ and fibronectin were labeled with rabbit antibody directed against $\alpha 5$ integrin cytoplasmic tail (AB1928, Millipore) and mouse anti-fibronectin Alexa Fluor® 488 (FN-3, eBioscience), respectively (overnight incubation at 4 °C). After washing in PBS-Tween 0.1%, tissue sections were incubated for 1 hour with appropriate secondary antibody (goat anti-rabbit IgG Alexa Fluor® 647, Invitrogen). Nuclei were counterstained with DAPI and coverslips were mounted onto tissue section using Permafluor Aqueous Mounting Medium (Fisher). Images were acquired using a confocal microscope as previously described.

Dual wide field/TIRF imaging

Dual Wide field/TIRF images were acquired using an iMIC microscope (Till Photonics) equipped with a Cobolt Dual Calypso Laser 491/532 nm, a monochromator

Polychrome V and an Olympus 60× TIRFM (1.45 NA) objective. A multiband filter set was used for excitation of DAPI, Alexa fluor 491 and Alexa fluor 568. Wide field and TIRF images were recorded on an EMCCD camera (Andor Technology) and analyzed using ImageJ software.

Statistical analysis

Data are reported as mean ± S.E.M. unless otherwise stated. Statistical analysis between samples was done by one way analysis of the variance (ANOVA) followed by Bonferroni post-test with the GraphPad Prism program. Significance level is controlled by 95% confidence interval.

Results

α5 integrin and FN are involved in U87MG cell cohesion

Multicellular tumor spheroid is an *in vitro* model used in numerous studies to mimic micro-tumors [38]. FN assembly can promote cell–cell adhesion and foster spheroid formation in various cell types [39,40] including U87MG glioma cells [13,32]. In CHO cells, this process involves the $\alpha5\beta1$ integrin [31,41]. We seek to assess the role of the FN receptor $\alpha5\beta1$ in glioma cell–cell adhesion. U87MG cells express $\alpha5\beta1$ integrin endogenously and were manipulated to increase or decrease the expression of the $\alpha5$ integrin subunit. Cells were sorted for various expressions of $\alpha5$ integrin. $\alpha5$, $\beta1$ and αv integrin expression was controlled by flow cytometry analysis (Fig. 1A, left panel). $\alpha5$ and $\beta1$ expression was further confirmed by immunoblot (Fig. 1A, right panel). For this study we consistently used the cell expressing the highest (U87 $\alpha5+$) and lowest (U87 $\alpha5-$) level of $\alpha5$ integrin.

Under conventional culture condition, upon reaching high cell density, $\alpha5$ integrin depletion significantly decreased the spontaneous formation of multicellular organoid (Fig. 1B). After 3 days of culture, cell growth was similar for both cells indicating that the absence of spheroids in U87 $\alpha5-$ cell culture was not due to a decrease in cell density (Fig. 1B). We next challenged U87 $\alpha5+$ and U87 $\alpha5-$ cells in spheroid formation from suspended cells. We monitored the kinetics of spheroid formation, *i.e.*, spheroid area and spherical form (roundness) to assess the role of $\alpha5$ integrin in cell aggregation and tissue compaction. As shown in Fig. 1C, initial cell aggregation (after 6 hours of incubation) was not dependent on $\alpha5$ expression level. At 24 hours, U87 $\alpha5+$ cells increased their compaction and adopted a regular circular shape whereas $\alpha5$ -depleted cells presented a delayed cell compaction and spheroid formation. This difference is no more observed after 48 hours. $\alpha5$ integrin involvement in U87 spheroid formation was further confirmed by antibody-mediated. As a control, function inhibition of αv integrin (another fibronectin receptor) had no impact on spheroid formation (Fig. 1D). Confocal microscopy was next used to reveal the distribution of $\alpha5$ integrin, $\beta1$ integrin and FN on 2-day-old spheroids. For staining $\alpha5$ integrin, we used a monoclonal antibody (clone Snaka51) that recognizes a LIBS (ligand-induced binding site) epitope on the calf1/calf2 domain of $\alpha5$ integrin and that is a reporter of $\alpha5\beta1$ integrin activation and binding to FN [42]. Confocal images of U87 $\alpha5+$ spheroids clearly show the localization of the ligand-occupied $\alpha5$ integrin at the cell/cell contact and in vesicular-like intracellular structures (Fig. 2). Low-level $\alpha5$ expressing cells present a faint staining, with some remaining cell surface labeling in only a fraction of the cells. Anti- $\beta1$ integrin antibody stained the cell membrane similarly in both cell lines. FN labeling revealed a dense fibrillar network of assembled FN between U87 $\alpha5+$ cells. FN fibrillogenesis was $\alpha5\beta1$ -dependent as depicted by FN-immunolabeling in U87 $\alpha5-$ spheroids. Accordingly, immunolabeling of FN in LN229 glioma spheroids revealed the presence of a dense fibrillary network on $\alpha5$ expressing cells. As shown in U87 cells,

$\alpha5$ -depletion on LN229 cells decreased FN assembly (Fig. S1). Consistent with previous published data [13,31,39,41], our results highlighted that $\alpha5\beta1$ integrin mediates FN fibrillogenesis in tumor sphere and can promote glioma cell–cell adhesion via $\alpha5\beta1$ /FN-mediated bridges.

Balance between $\alpha5$ -mediated cell–cell and cell–substratum adhesion directs U87 evasion

FN-mediated cell/cell cohesion has been associated with a decrease in cell dispersion from prostate tumor spheroids, suggesting that $\alpha5\beta1$ may have anti-invasive function [32]. To confirm this observation on glioma cells, we examined the effect of $\alpha5$ integrin expression on spheroid evasion, a model of collective migration. In the first set of experiments, U87 spheroids were deposited onto poly-L-lysine coated plates. Phase contrast images (Fig. 3A) and image analysis show that $\alpha5$ integrin depletion or its functional inhibition significantly increased the number of evading cells (Fig. 3B) but had no effect on the mean distance of migration from the spheroids (Fig. 3C). Similar data were obtained using clonal population of LN229 GBM cells genetically manipulated to express various amount of $\alpha5$ integrin (Fig. S1). Inhibition of αv integrin suppressed U87 cell evasion and migration in all experimental conditions. Since αv inhibition had no impact on spheroid formation (Fig. 1D), these data suggested that migration on poly-L-lysine did not require $\alpha5$ integrin but was αv -dependent. The non-receptor tyrosine kinase FAK (focal adhesion kinase) is an essential marker of focal adhesions and is phosphorylated on tyr397 upon its recruitment by integrins [43]. After immunolabeling the migrating cells, confocal images show the localization of αv integrin in pFAK-tyr397 positive focal adhesion (FA), supporting for a functional role of this integrin in U87 $\alpha5-$ cell dispersion on poly-L-lysine (Fig. S2). Taken together, these data are in line with those from Reference 32, suggesting that $\alpha5$ integrin/FN mediated cell–cell adhesion may impede cell dispersion from tumor mass.

However, cell dispersion from multicellular aggregates is regulated by opposite forces produced by cell–cell adhesion and ECM mediated cell migration [44,45]. In such a case, the presence of FN in the surrounding microenvironment would engage $\alpha5\beta1$ integrin in cell–substratum interaction and challenge FN-mediated cell–cell adhesion. To test this hypothesis, we examined cell dispersion of U87 spheres plated on wells coated with increasing amounts of FN. Phase-contrast images (Fig. 4A) and image quantification (Fig. 4B and C) showed that U87 $\alpha5+$ cell dissemination was dependent on FN concentration. By contrast, evasion and migration of U87 $\alpha5-$ cells were not stimulated by the presence of FN in spheroid microenvironment. To assess the integrin involved in cell evasion and migration from the spheroid, we used function blocking antibodies on spheroid plated on FN-rich substratum. In this case, the number of U87 $\alpha5+$ cells evading cells and their distance of migration were $\alpha5\beta1$ -dependent and did not require functional αv (Fig. 4D, left panels). By contrast, for U87 $\alpha5-$ cells, the number of evaded cells was inhibited by anti- αv antibody and to a lesser extent by anti- $\alpha5$ antibody, and their distance of migration was strictly dependent of αv integrin and not of the $\alpha5$ integrin (Fig. 4D, right panels). Involvement of αv integrin in U87 $\alpha5-$ cell migration was further confirmed by immunostaining of αv integrin and pFAK-tyr397. Our data clearly show the presence of mature FAs containing both αv integrin and pFAK-tyr397 on U87 $\alpha5-$ cells that migrated at great distances away from spheroids (Fig. S2). Altogether, these results highlight that changes in FN concentration in the tumor sphere microenvironment regulate the balance between $\alpha5$ integrin-mediated cell–cell and cell–substratum adhesion, and as a consequence, U87 cell dissemination.

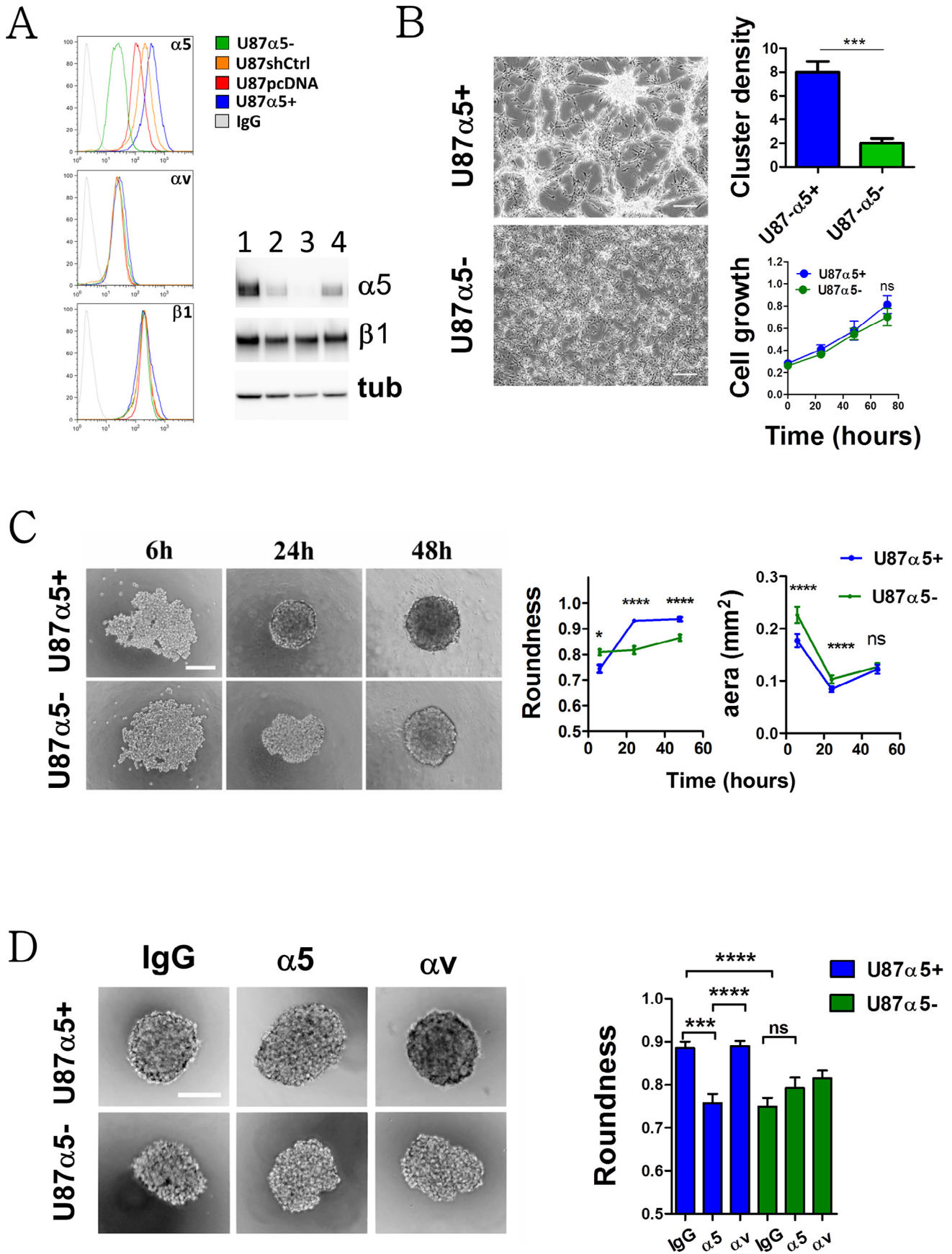


Fig. 1. 87 cells expressing high (U87 α 5+) or low (U87 α 5-) amount of α 5 integrin were analyzed to show the involvement of α 5 in cell–cell adhesion. (A) Left panel – analyzed by flow cytometry of α 5, α v, β 1 cell surface expression on U87 cells manipulated to overexpress or repress α 5 integrin. Right panel – confirmation by immunoblot of α 5 and β 1 expression level on the U87 cell lines: lane 1, U87 α 5+; lane2, U87pcDNA, lane3, U87 α 5-; lane4, U87shCtrl. (B) Phase contrast images of U87 cells cultured for 4 days under conventional conditions. Scale bar: 200 μ m. The number of cell clusters per field was manually counted. Data presented are the mean \pm s.e.m. of 3 different experiments (4 fields/experiments). U87 cells were cultured for 3 days on plastic dishes and cell growth was monitored as described in Material and methods. (C) Left panel – phase contrast images of U87 cell spheroid for the indicated period of time in non-adherent U-shaped wells (2000 cells/well). Right panel – morphological parameters (area and roundness) of each spheroid were measured using ImageJ software. (D) Spheroids were formed for 18 h in the presence of irrelevant IgG or function-blocking antibodies targeting α 5 or α v integrins (10 μ g/mL each) and spheroid roundness was monitored. Data are the mean \pm s.e.m. of 15–20 spheroids from 3 independent experiments. * p < 0.05; ** p < 0.01; *** p < 0.001; **** p < 0.0001.

Remodeling of α 5 integrin adhesion during cell evasion from spheroid

To gain insight into the role of α 5 β 1 in cell–cell interaction and during cell evasion from tumor organoid, we examined by confocal microscopy, the distribution of ligand-occupied α 5 integrin and FN. In the first series of images (Fig. 5A), focal planes were selected at a distance of 5 μ m above the coverslips at the margin of the spheroid (indicated by the dashed lines in the figures). As U87 α 5+ cells emerged from the spheroid, α 5 integrin depicted a pattern with thin and long fibrils. 3D reconstruction of whole z-stacks showed that ligand-occupied α 5 is clearly around the cells (Fig. S3). Moreover, a dense fibrillar network of assembled FN was clearly visible. In α 5-depleted glioma cells evaded from the spheroid did not form any FN network (Fig. 5A). To confirm these results, we used LN443, another GBM cell line expressing a high level of α 5 integrin (Fig. S2). In LN443 cells, activated- α 5 integrin depicted a similar pattern to that of U87 α 5+ cells (Figs. S4 and S5). We also observed a dense network of assembled FN surrounding emerging LN443 cells (Figs. S6 and S7). To assess the presence of fibrillogenesis *in vivo*, FN and α 5 integrin distribution were examined by confocal immunofluorescence on paraffin embedded tissue sections of human tumor xenografts. Interestingly, we found numerous areas presenting dense FN fibrillary network and strong α 5 immunoreactivity (Fig. S8), confirming the relevance of fibrillary FN in GBM models. These observations indicated that glioma cells evaded collectively from the spheroid. During this process, α 5 integrin maintained cell–cell interaction in fibrillar-like adhesions. To the best of our knowledge, this is the first description of this kind of adhesive structure.

To examine the organization of α 5 integrin and of its ligand at the cell–substratum level, a second series of confocal images was taken on the same microscopic fields, but at a focal plane corresponding to the cell–substratum interface (Fig. 5B). Matrix-bound

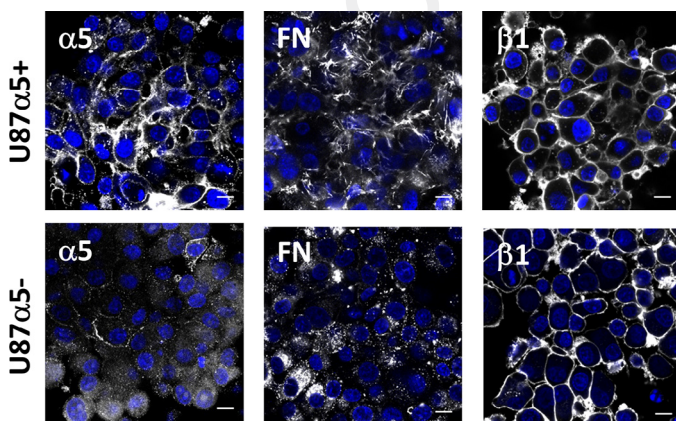


Fig. 2. Distribution of α 5, β 1 integrins and fibronectin in U87 cell spheroids. Suspended spheroids were immunolabeled as described in Material and methods. Confocal images were taken at an optical section between 10 μ m and 20 μ m above the base of the spheroid. Note the increase amount of fibrils in U87 α 5+ cells. Nuclei were stained with DAPI. Bar = 20 μ m.

α 5 integrin exhibited a pattern clearly distinguishable to that of cell–cell fibrillar adhesions. The integrin was distributed in thin dots with some elongated labeling resembling small fibrils (arrow heads). These integrin adhesion sites were morphologically distinct from classical focal adhesions (FAs, Fig. 6C). The presence of thin and short FN fibrils (arrow heads) indicated a reduced FN assembly at the substratum level compared to the one observed at cell–cell interaction level. In our experimental settings, coated FN was also immunodetected. The loss of immunoreactivity under the spheroid and under the evading cells likely reflected an intense matrix remodeling. In U87 α 5- cells, FN assembly was further decreased and FN remodeling was less pronounced. Together, these experiments described that glioma cells may maintain contact with their neighbor during collective evasion using α 5 integrin and assembled FN.

α 5 integrin does not colocalize with pFAK-tyr397 in cell–cell fibrillar adhesion

By confocal microscopy, we examined α 5 and pFAK-tyr397 colocalization on U87 α 5+ and LN443 glioma cells. Surprisingly, in cells that collectively emerged from the spheroid, pFAK-tyr397 was distributed as punctate intracellular clusters (Figs. 6A and S4A) of size smaller than the classical FAs (Fig. 6C and D). Image quantification showed that in U87 cells, pFAK-tyr397 did not colocalize with FN-bound α 5 integrin (Fig. 6E). The absence of colocalization between pFAK-tyr397 and α 5 integrin at cell–cell junction was also observed on confocal images of U87 α 5+ suspended spheroids (Fig. S9). Altogether, these data indicate that pFAK-tyr397 was not associated with cell–cell fibrillary adhesion. At the substratum level of glioma cells close to spheroids (Figs. 6B and S4B), pFAK-tyr397 was also found in small punctate cluster (Fig. 6D) that did not colocalize with α 5 integrin (Fig. 6E). Classical labeling of FAs and strong colocalization between α 5 integrin and pFAK-tyr397 were found in cells that had migrated to long distances from the tumor sphere (Figs. 6C, E and S4, arrow heads). α 5 integrin was also detected in thin classical fibrillar adhesions characterized by the absence of pFAK-tyr397 (Figs. 6C and S4C, arrows).

The previous experiments suggest that classical FAs were progressively formed as glioma cells migrated away from the spheroids. To further confirm this observation, we examined α 5 integrin adhesion reorganization at the substratum level using total internal reflection microscopy (TIRF). Dual color wide field TIRF experiments confirmed the presence of a punctate pFAK-tyr397 staining in cells localized beneath and in close proximity of the spheroid, suggesting that they were not able to assemble mature FAs. Integrin α 5 was not found with these punctuate structures but was rather associated with cell–cell contacts and/or fibronectin fibrils as suggested by the elongated form of the staining (Fig. 7A and B). On the other hand, when cells migrated away from the spheroid, colocalization of integrin α 5 and pFAK-tyr397 at focal complexes and focal adhesions could be observed (Fig. 7C). Our data showed that cell–cell fibrillar adhesion did not contain activated FAK and that classical α 5-containing FAs are progressively formed during the process of cell migration.

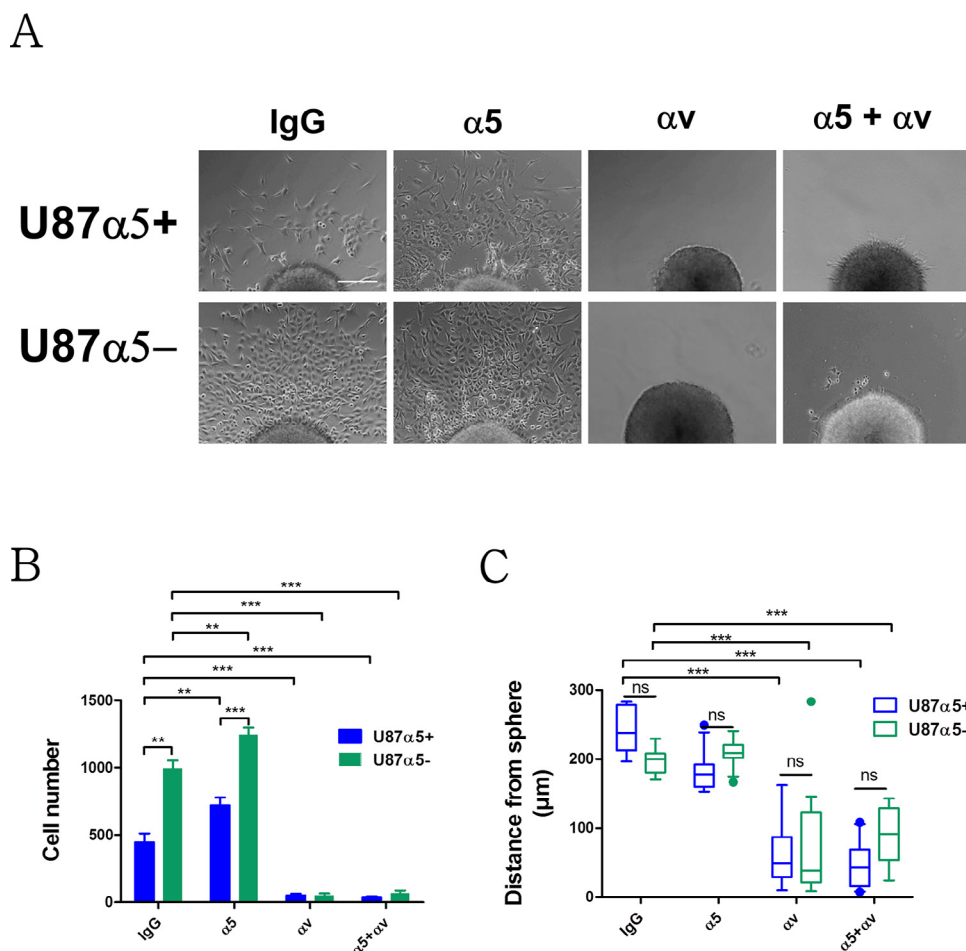


Fig. 3. Two-day old spheroids were plated onto poly-L-lysine coated plastic dishes in the presence of irrelevant IgG or function-blocking antibodies targeting $\alpha 5$ or αv integrins (10 $\mu\text{g}/\text{mL}$ each). (A) Phase contrast images of representative spheroids after 24 hours of migration. Scale bar = 100 μm . (B) After DAPI staining, the number of evading cells were quantified by automated counting of nuclei using ImageJ software and plotted as the mean \pm s.e.m. (C) The distance of migration from the spheroid was measured for each cell and the mean distance was calculated for each spheroid. Data are plotted as Tukey box and whiskers. 15 spheroids from 3 independent experiments were used per condition. ** $p < 0.05$; *** $p < 0.001$.

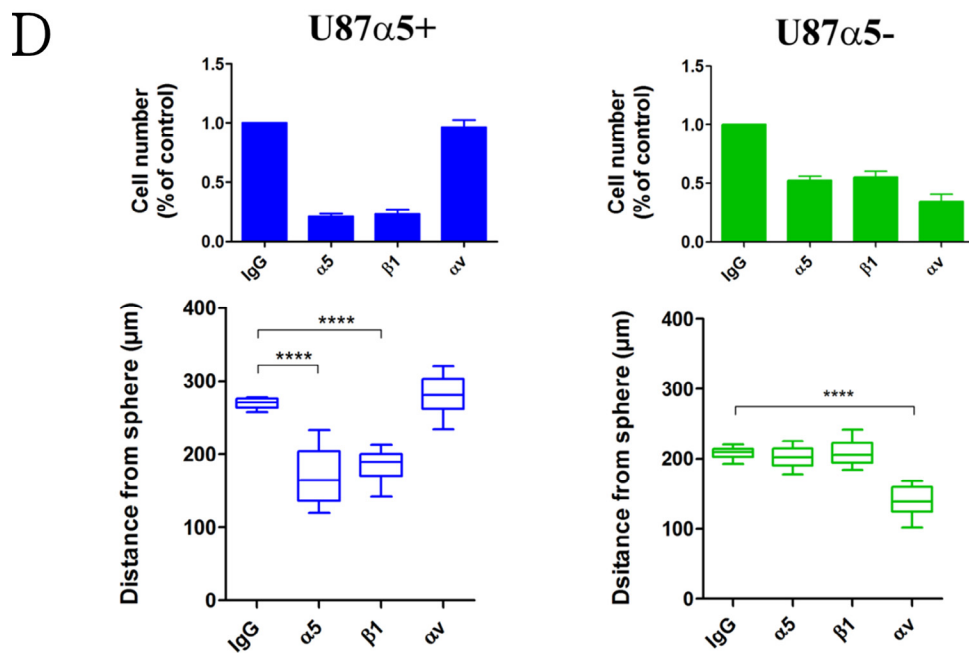
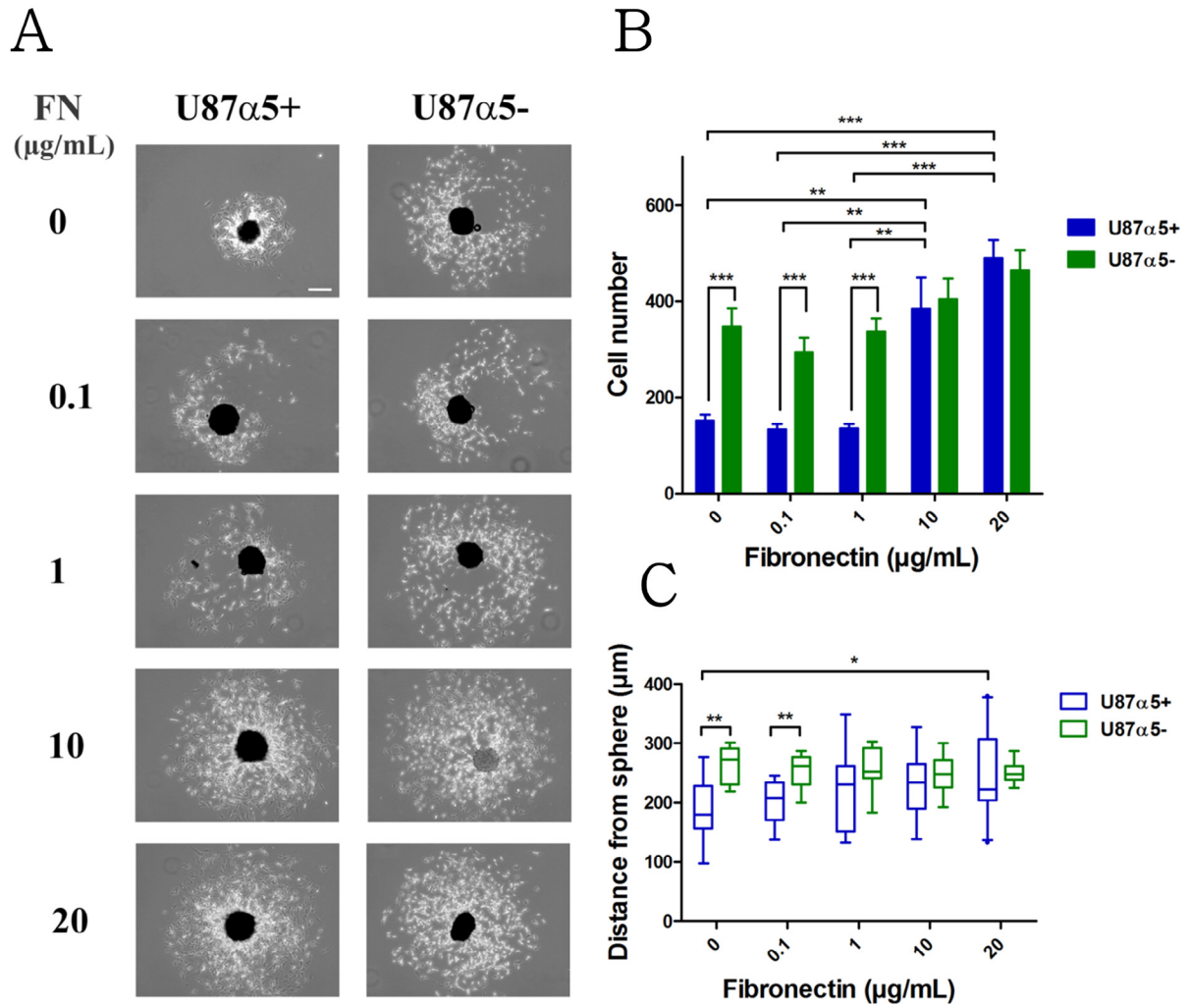
Discussion

Highly efficient infiltration in the surrounding brain parenchyma is a hallmark of glioblastoma cells and a major cause of therapy failure. A better understanding of GBM cell invasive behavior is urgently needed to improve therapeutic approaches to fight these tumors [2]. In the present work, we intended to clarify the function of $\alpha 5$ integrin, the fibronectin receptor, in GBM spheroid formation and in cell dispersion. We found that ligand-occupied $\alpha 5$ integrin can be localized in fibrillar adhesion at cell-cell interaction. These results exemplify the molecular and morphological diversity and the plasticity of $\alpha 5$ adhesions engaged both in cell-cell and cell-substratum interactions. We showed that cell evasion from tumor sphere is regulated by a balance between $\alpha 5$ -mediated cell-cell and cell-substratum interactions. In clinical situation, GBM frequently overexpressed FN that is found in fibrillar deposit in the tumor [12]. High level of FN expression will thus promote $\alpha 5\beta 1$ -

mediated glioma cell dissemination from the tumor mass. In such case patients would benefit from anti- $\alpha 5$ integrin therapy.

Multicellular tumor spheroids are three dimensional (3D) architecture that mimic avascular tumor areas comprising the establishment of diffusion gradients, reduced proliferation rates and increased drug resistance. They are increasingly used as an improvement of conventional 2D culture systems as they offer 3D *in vivo*-like environment as well as cell-ECM and cell-cell interactions. Spheroid formation from a cell suspension is a multistep process that required cell aggregation and tension force mediated cell compaction [46]. The present work illustrated that $\alpha 5\beta 1$ and cell-mediated FN fibrillogenesis play a pivotal role in glioma spheroid formation. Time course experiments indicated that $\alpha 5\beta 1$ expression level has no impact on the early phase of spheroid formation. This is in line with other studies [47,48] showing that integrins are not involved in cell aggregation but rather promote the condensation phase of the spheroid formation. In agreement

Fig. 4. (A) Two-day-old spheroids were plated on plastic dishes coated with indicated amount of fibronectin (FN). Phase contrast images were taken 24 hours after spheroid seeding. Scale bar = 200 μm . (B) After DAPI staining, cell evasion was quantified and mean number of evading cells was plotted \pm s.e.m. (C) The distance of migration from the spheroid was measured for each cell and the mean distance was calculated for each spheroid. Data are plotted as box and whiskers (min-max). (D) Spheroids were plated on plastic dishes coated with fibronectin in the presence of irrelevant IgG or function-blocking antibodies targeting $\alpha 5$, $\beta 1$ or αv integrins (10 $\mu\text{g}/\text{mL}$ each). Data are the mean cell number \pm s.e.m. and the mean distance of cell migration per spheroid plotted as box and whiskers (min-max) - 12 to 18 spheroids from 4 independent experiments were analyzed. * $p < 0.05$; ** $p < 0.01$; *** $p < 0.001$.



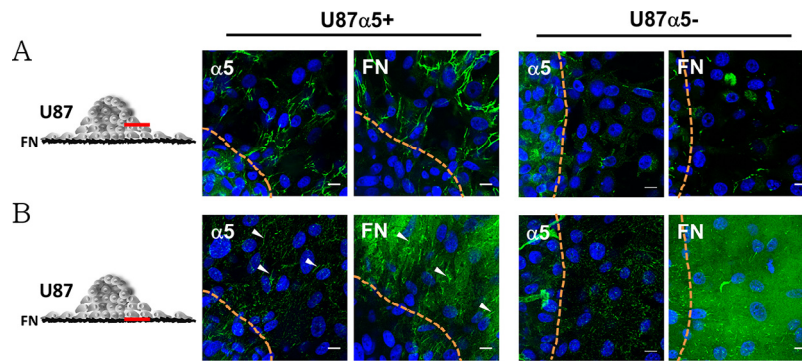


Fig. 5. Two-day-old spheroids were plated on FN-coated (10 $\mu\text{g}/\text{mL}$) glass coverslips. 18 hours later, cells were fixed and immunolabeled to detect ligand-occupied $\alpha 5$ integrin ($\alpha 5$) and fibronectin (FN) as described in Material and methods. Confocal images were taken at 2 different zones as depicted in the diagrams to examine (A) cells emerging from the tumor sphere at a focal plane 5 μm above the coverslips and (B) same microscopic field but at a focal plane corresponding to the substratum. Orange dotted lines indicate the border of the spheroid. Arrow heads = fibrillar adhesion. Scale bar = 10 μm .

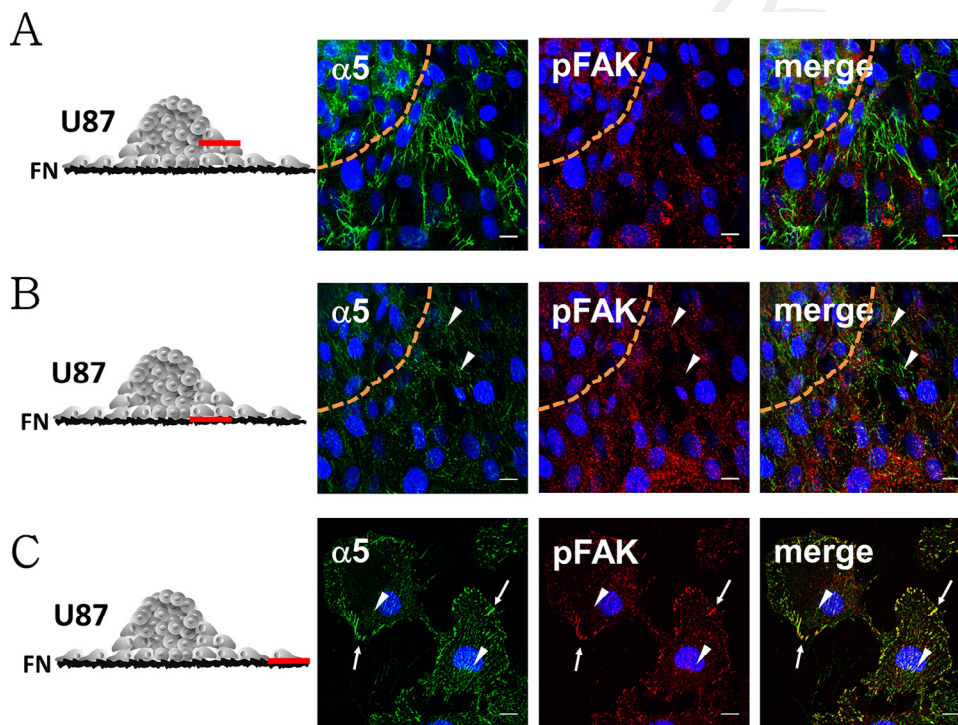


Fig. 6. Two-day-old U87 $\alpha 5+$ spheroids were plated on FN-coated (10 $\mu\text{g}/\text{mL}$) glass coverslips. 18 hours later, cells were fixed and ligand-occupied $\alpha 5$ integrin ($\alpha 5$) and pFAK-tyr397 (pFAK) were immunodetected. Confocal images were taken at 3 different zones as depicted in the diagrams to examine (A) cells emerging from the tumor sphere at a focal plane 5 μm above the coverslips, (B) same microscopic field but at a focal plane corresponding to the substratum and (C) cell/substratum interface of cells that migrated away from the sphere. (D) Quantitative image analysis of pFAK-tyr397 cluster size was performed as described in Material and methods. Data are presented as the mean Feret diameters of each individual image ($n = 8-12$) from 2 independent experiments. (E) Integrin/pFAK-tyr397 colocalization was evaluated using Pearson's correlation coefficient. 10-12 images from 2 experiments were used. **** $p < 0.0001$. Orange dotted lines indicate the border of spheroids. Arrow heads = fibrillar adhesions; arrows = focal contacts. Scale bar = 10 μm .

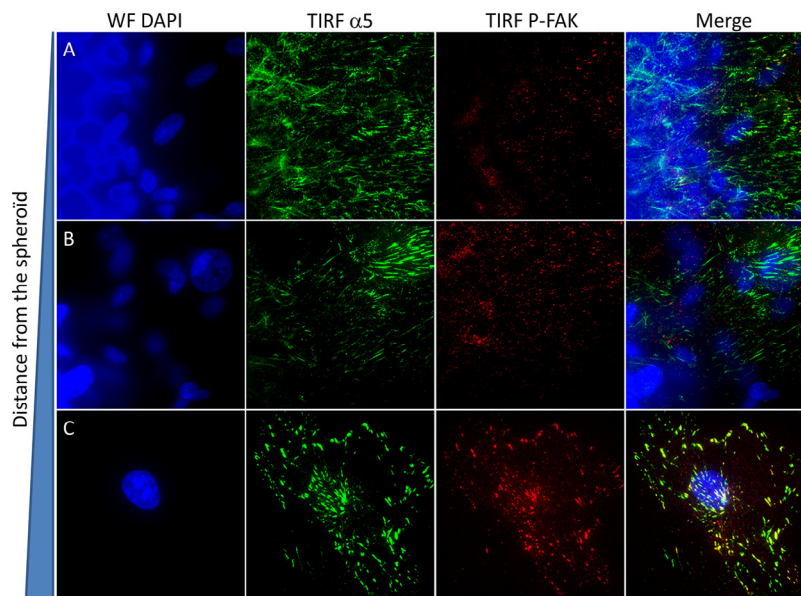


Fig. 7. Two-day-old U87 α 5+ spheroids were plated on FN-coated (10 μ g/mL) glass coverslips in complete medium for 18 hours. Fixed cells were immunolabeled using anti- α 5 and rabbit anti-pFAKtyr397 antibodies. Dual color wide field TIRF images were acquired at increasing distances from the spheroid.

with previous published data [13,31–33,40,41,49], it is likely that, in tumor cell aggregates, α 5-mediated cell tension and contractility promotes FN assembly and cell–cell interaction.

An important observation of our work is that during their collective evasion from tumor sphere, glioma cells maintained contacts with their neighbor using cell–cell fibrillar adhesions. In line with previous studies comparing FN fibrillogenesis in 2D and 3D cell cultures [50–52], we observed that fibrillar FN networks were much more developed at cell–cell interaction than at cell–substratum level. In our experimental model, α 5 integrin relocalized at cell substratum adhesion sites and progressively formed mature FAs as cells migrated at distance from the spheroid, requiring FN matrix remodeling and turnover. It has been shown that RhoA signaling pathway and inverted formin 2 promote fibrillary adhesion and FN matrix assembly [53–57]. Conversely, the caveolin-1 and RAS-RAF signaling pathway inhibit FN fibrillogenesis [52,58]. FN fibrils turnover is also regulated by extracellular proteins such as transglutaminase 2 or the membrane type matrix metalloproteinase 1 [12,59,60]. Future experiments will help to decipher molecular pathways involved in cell–cell fibrillar adhesion turnover during glioma cell dissemination. In this context, cell dispersion from spheroids represents a useful model to study the dynamics of α 5 integrin adhesion sites and fibrillar FN remodeling that may take place during glioma cell invasion *in vivo*.

Our data indicate that α 5 integrin can trigger cell–cell interaction and FN fibrillogenesis independently of pFAK-tyr397 recruitment. At cell–substratum level, pFAK-tyr397 was poorly associated with ligand-bound α 5 integrin on cells close to the spheroid. pFAK-tyr397/integrin association was progressively detectable on migrating cells. This observation suggests that α 5 integrin engagement at cell–cell contact may regulate cell–substratum interaction by inhibiting pFAK-tyr397 recruitment at the plasma membrane and therefore FAs formation and maturation. In glioblastoma, α 5 β 1 integrin may thus not always be associated with pFAK-tyr397 and their interaction may be finely regulated by the balance between cell–cell and cell–substratum interactions. For instance, *in situ* analysis revealed that in glioblastoma, co-expression of β 1 integrin and pFAK-tyr397 was detected in morphologically defined regions such as perivascular or tumor infiltration zones and not in the tumor mass [61].

In the present work, we described for the first time cell–cell fibrillar adhesions as pFAK-tyr397-independent α 5 adhesion sites involved in glioma cell–cell interactions. A recent study demonstrated that α 5 integrin can foster cell–cell adhesion by an alternative mechanism, involving direct interaction between inactive integrins expressed by adjacent cells [62]. In light of these new data, it appears that α 5 integrin function is not restricted to cell–substratum adhesion and that its involvement in glioma and in other solid cancers progression may deserve a reevaluation. We and others have shown that α 5 integrins play a critical role in glioma resistance to radio- and chemo-therapy. It will be important in the future to characterize the composition, the regulation and the function of cell–cell fibrillar adhesions in order to better assess its involvement in glioma progression and resistance to therapy. In this context, our experimental model will be useful for the design of new effective strategies for fighting GBM.

Acknowledgements

We thank Pr José Luis and Dr. Sylvie Thuault for their technical expertise. This work was supported by the University of Strasbourg, the Ligue Contre le Cancer (Comité du Grand Est), the Cancéropole Grand Est and the Region Alsace – Program INTEGLIO, the Henri Curien Partnerships – Program Balaton and University of Strasbourg-Program IDEX. Anne-Florence Blandin and Guillaume Renner are doctoral fellows from the French Ministère de l'Enseignement Supérieur et de la Recherche.

Conflict of interest

None.

Appendix: Supplementary material

Supplementary data to this article can be found online at [doi:10.1016/j.canlet.2016.04.007](https://doi.org/10.1016/j.canlet.2016.04.007).

References

- [1] M. Nakada, S. Nakada, T. Demuth, N.L. Tran, D.B. Hoelzinger, M.E. Berens, Molecular targets of glioma invasion, *Cell. Mol. Life Sci.* 64 (2007) 458–478, doi:10.1007/s00018-007-6342-5.
- [2] A. Vehlou, N. Cordes, Invasion as target for therapy of glioblastoma multiforme, *Biochim. Biophys. Acta* 2013 (1836) 236–244, doi:10.1016/j.bbcan.2013.07.001.
- [3] V. Montana, H. Sontheimer, Bradykinin promotes the chemotactic invasion of primary brain tumors, *J. Neurosci.* 31 (2011) 4858–4867, doi:10.1523/JNEUROSCI.3825-10.2011.
- [4] E. Hirata, H. Yukinaga, Y. Kamioka, Y. Arakawa, S. Miyamoto, T. Okada, et al., In vivo fluorescence resonance energy transfer imaging reveals differential activation of Rho-family GTPases in glioblastoma cell invasion, *J. Cell Sci.* 125 (2012) 858–868, doi:10.1242/jcs.089995.
- [5] A.C. Bellail, S.B. Hunter, D.J. Brat, C. Tan, E.G. Van Meir, Microregional extracellular matrix heterogeneity in brain modulates glioma cell invasion, *Int. J. Biochem. Cell Biol.* 36 (2004) 1046–1069, doi:10.1016/j.biocel.2004.01.013.
- [6] D.J. Silver, F.A. Siebzehnrubl, M.J. Schildts, A.T. Yachnis, G.M. Smith, A.A. Smith, et al., Chondroitin sulfate proteoglycans potently inhibit invasion and serve as a central organizer of the brain tumor microenvironment, *J. Neurosci.* 33 (2013) 15603–15617, doi:10.1523/JNEUROSCI.3004-12.2013.
- [7] A. Lal, A.E. Lash, S.F. Altschul, V. Velculescu, L. Zhang, R.E. McLendon, et al., A public database for gene expression in human cancers, *Cancer Res.* 59 (1999) 5403–5407.
- [8] P. Castellani, L. Borsi, B. Carnemolla, A. Birò, A. Dorcaratto, G.L. Viale, et al., Differentiation between high- and low-grade astrocytoma using a human recombinant antibody to the extra domain-B of fibronectin, *Am. J. Pathol.* 161 (2002) 1695–1700.
- [9] R. Mahesparan, T.-A. Read, M. Lund-Johansen, K.O. Skaftnesmo, R. Bjerkvig, O. Engebraaten, Expression of extracellular matrix components in a highly infiltrative in vivo glioma model, *Acta Neuropathol.* 105 (2003) 49–57, doi:10.1007/s00401-002-0610-0.
- [10] E. Serres, F. Debarbieux, F. Stanchi, L. Maggiorella, D. Grall, L. Turchi, et al., Fibronectin expression in glioblastomas promotes cell cohesion, collective invasion of basement membrane in vitro and orthotopic tumor growth in mice, *Oncogene* 33 (2014) 3451–3462, doi:10.1038/ncr.2013.305.
- [11] T. Ohnishi, S. Hiraga, S. Izumoto, H. Matsumura, Y. Kanemura, N. Arita, et al., Role of fibronectin-stimulated tumor cell migration in glioma invasion in vivo: clinical significance of fibronectin and fibronectin receptor expressed in human glioma tissues, *Clin. Exp. Metastasis* 16 (1998) 729–741, doi:10.1023/A:1006532812408.
- [12] L. Yuan, M. Siegel, K. Choi, C. Khosla, C.R. Miller, E.N. Jackson, et al., Transglutaminase 2 inhibitor, KCC009, disrupts fibronectin assembly in the extracellular matrix and sensitizes orthotopic glioblastomas to chemotherapy, *Oncogene* 26 (2007) 2563–2573, doi:10.1038/sj.onc.1210048.
- [13] E. Serres, F. Debarbieux, F. Stanchi, L. Maggiorella, D. Grall, L. Turchi, et al., Fibronectin expression in glioblastomas promotes cell cohesion, collective invasion of basement membrane in vitro and orthotopic tumor growth in mice, *Oncogene* 33 (2013) 3451–3462, doi:10.1038/ncr.2013.305.
- [14] S. Sengupta, S. Nandi, E.S. Hindi, D.A. Wainwright, Y. Han, M.S. Lesniak, Short hairpin RNA-mediated fibronectin knockdown delays tumor growth in a mouse glioma model, *Neoplasia* 12 (2010) 837.
- [15] T. Ohnishi, N. Arita, S. Hiraga, T. Taki, S. Izumoto, Y. Fukushima, et al., Fibronectin-mediated cell migration promotes glioma cell invasion through chemokinetic activity, *Clin. Exp. Metastasis* 15 (1997) 538–546.
- [16] A.-F. Blandin, G. Renner, M. Lehmann, I. Lelong-Rebel, S. Martin, M. Dontenwill, $\beta 1$ integrins as therapeutic targets to disrupt hallmarks of cancer, *Front Pharmacol.* (2015) 279, doi:10.3389/fphar.2015.00279.
- [17] M.C. Gingras, E. Roussel, J.M. Bruner, C.D. Branch, R.P. Moser, Comparison of cell adhesion molecule expression between glioblastoma multiforme and autologous normal brain tissue, *J. Neuroimmunol.* 57 (1995) 143–153.
- [18] E.C. Cosset, J. Godet, N. Entz-Werlé, E. Guérin, D. Guenot, S. Froelich, et al., Involvement of the TGF β pathway in the regulation of $\alpha 5$ $\beta 1$ integrins by caveolin-1 in human glioblastoma, *Int. J. Cancer* 131 (2012) 601–611, doi:10.1002/ijc.26415.
- [19] H. Janouskova, A. Maglott, D.Y. Leger, C. Bossert, F. Noulet, E. Guerin, et al., Integrin $\alpha 5 \beta 1$ plays a critical role in resistance to temozolomide by interfering with the p53 pathway in high-grade glioma, *Cancer Res.* 72 (2012) 3463–3470, doi:10.1158/0008-5472.CAN-11-4199.
- [20] K.M. Holmes, M. Annala, C.Y.X. Chua, S.M. Dunlap, Y. Liu, N. Hugen, et al., Insulin-like growth factor-binding protein 2-driven glioma progression is prevented by blocking a clinically significant integrin, integrin-linked kinase, and NF- κ B network, *Proc. Natl. Acad. Sci. U.S.A.* 109 (2012) 3475–3480, doi:10.1073/pnas.1120375109.
- [21] J.D. Lathia, M. Li, M. Sinyuk, A.G. Alvarado, W.A. Flavahan, K. Stoltz, et al., High-throughput flow cytometry screening reveals a role for junctional adhesion molecule a as a cancer stem cell maintenance factor, *Cell Rep.* 6 (2014) 117–129, doi:10.1016/j.celrep.2013.11.043.
- [22] D.M. Mallawaarachy, M.E. Buckland, K.L. McDonald, C.C.Y. Li, L. Ly, E.K. Sykes, et al., Membrane proteome analysis of glioblastoma cell invasion, *J. Neuropathol. Exp. Neurol.* 74 (2015) 425–441, doi:10.1097/NEN.0000000000000187.
- [23] F. Schaffner, A.M. Ray, M. Dontenwill, Integrin $\alpha 5 \beta 1$, the fibronectin receptor, as a pertinent therapeutic target in solid tumors, *Cancers (Basel)* 5 (2013) 27–47, doi:10.3390/cancers5010027.
- [24] G. Renner, H. Janouskova, F. Noulet, V. Koenig, E. Guerin, S. Bär, et al., Integrin $\alpha 5 \beta 1$ and p53 convergent pathways in the control of anti-apoptotic proteins PEA-15 and survivin in high-grade glioma, *Cell Death Differ.* 23 (2015) 640–653, doi:10.1038/cdd.2015.131.
- [25] E. Martinkova, A. Maglott, D.Y. Leger, D. Bonnet, M. Stiborova, K. Takeda, et al., $\alpha 5 \beta 1$ integrin antagonists reduce chemotherapy-induced premature senescence and facilitate apoptosis in human glioblastoma cells, *Int. J. Cancer* 127 (2010) 1240–1248, doi:10.1002/ijc.25187.
- [26] J.E. Schwarzbauer, D.W. DeSimone, Fibronectins, their fibrillogenesis, and in vivo functions, *Cold Spring Harb. Perspect. Biol.* 3 (2011) a005041, doi:10.1101/cshperspect.a005041.
- [27] B.-Z. Katz, E. Zamir, A. Bershadsky, Z. Kam, K.M. Yamada, B. Geiger, Physical state of the extracellular matrix regulates the structure and molecular composition of cell-matrix adhesions, *Mol. Biol. Cell* 11 (2000) 1047–1060, doi:10.1091/mbc.11.3.1047.
- [28] R. Pankov, E. Kucierman, B.-Z. Katz, K. Matsumoto, D.C. Lin, S. Lin, et al., Integrin dynamics and matrix assembly tensin-dependent translocation of $\alpha 5 \beta 1$ integrins promotes early fibronectin fibrillogenesis, *J. Cell Biol.* 148 (2000) 1075–1090, doi:10.1083/jcb.148.5.1075.
- [29] A.-M. Ray, F. Schaffner, H. Janouskova, F. Noulet, D. Rognan, I. Lelong-Rebel, et al., Single cell tracking assay reveals an opposite effect of selective small non-peptidic $\alpha 5 \beta 1$ or $\alpha \beta 3 / \beta 5$ integrin antagonists in U87MG glioma cells, *Biochim. Biophys. Acta* 1840 (2014) 2978–2987, doi:10.1016/j.bbagen.2014.04.024.
- [30] S. Martin, E.C. Cosset, J. Terrand, A. Maglott, K. Takeda, M. Dontenwill, Caveolin-1 regulates glioblastoma aggressiveness through the control of $\alpha 5 \beta 1$ integrin expression and modulates glioblastoma responsiveness to SJ749, an $\alpha 5 \beta 1$ integrin antagonist, *Biochim. Biophys. Acta* 1793 (2009) 354–367, doi:10.1016/j.bbamer.2008.09.019.
- [31] E.E. Robinson, R.A. Foty, S.A. Corbett, Fibronectin matrix assembly regulates $\alpha 5 \beta 1$ -mediated cell cohesion, *Mol. Biol. Cell* 15 (2004) 973–981, doi:10.1091/mbc.E03-07-0528.
- [32] J. Sabari, D. Lax, D. Connors, I. Brotman, E. Mindrebo, C. Butler, et al., Fibronectin matrix assembly suppresses dispersal of glioblastoma cells, *PLoS ONE* 6 (2011) e24810, doi:10.1371/journal.pone.0024810.
- [33] P. Singh, J.E. Schwarzbauer, Fibronectin matrix assembly is essential for cell condensation during chondrogenesis, *J. Cell Sci.* 127 (2014) 4420–4428, doi:10.1242/jcs.150276.
- [34] M. Lehmann, C. Rabenandrasana, R. Tamura, J.C. Lissitzky, V. Quaranta, J. Pichon, et al., A monoclonal antibody inhibits adhesion to fibronectin and vitronectin of a colon carcinoma cell line and recognizes the integrins $\alpha v \beta 3$, $\alpha v \beta 5$, and $\alpha v \beta 6$, *Cancer Res.* 54 (1994) 2102–2107.
- [35] L. Carduner, R. Agniel, S. Kellouche, C.R. Picot, C. Blanc-Fournier, J. Leroy-Dudal, et al., Ovarian cancer ascites-derived vitronectin and fibronectin: combined purification, molecular features and effects on cell response, *Biochim. Biophys. Acta* 1830 (2013) 4885–4897, doi:10.1016/j.bbagen.2013.06.023.
- [36] C.A. Schneider, W.S. Rasband, K.W. Eliceiri, NIH image to ImageJ: 25 years of image analysis, *Nat. Methods* 9 (2012) 671–675, doi:10.1038/nmeth.2089.
- [37] S. Bolte, F.P. Cordelières, A guided tour into subcellular colocalization analysis in light microscopy, *J. Microsc.* 224 (2006) 213–232, doi:10.1111/j.1365-2818.2006.01706.x.
- [38] F. Hirschhaeuser, H. Menne, C. Dittfeld, J. West, W. Mueller-Klieser, L.A. Kunz-Schughart, Multicellular tumor spheroids: an underestimated tool is catching up again, *J. Biotechnol.* 148 (2010) 3–15, doi:10.1016/j.jbiotec.2010.01.012.
- [39] D. Jia, I. Entersz, C. Butler, R.A. Foty, Fibronectin matrix-mediated cohesion suppresses invasion of prostate cancer cells, *BMC Cancer* 12 (2012) 94, doi:10.1186/1471-2407-12-94.
- [40] P. Salmenperä, E. Kankuri, J. Bizik, V. Sirén, I. Virtanen, S. Takahashi, et al., Formation and activation of fibroblast spheroids depend on fibronectin-integrin interaction, *Exp. Cell Res.* 314 (2008) 3444–3452, doi:10.1016/j.jyexcr.2008.09.004.
- [41] E.E. Robinson, K.M. Zazzali, S.A. Corbett, R.A. Foty, $\alpha 5 \beta 1$ integrin mediates strong tissue cohesion, *J. Cell Sci.* 116 (2003) 377–386, doi:10.1242/jcs.00231.
- [42] K. Clark, R. Pankov, M.A. Travis, J.A. Askari, A.P. Mould, S.E. Craig, et al., A specific $\alpha 5 \beta 1$ -integrin conformation promotes directional integrin translocation and fibronectin matrix formation, *J. Cell Sci.* 118 (2005) 291–300, doi:10.1242/jcs.01623.
- [43] A. Hamadi, M. Bouali, M. Dontenwill, H. Stoeckel, K. Takeda, P. Rondé, Regulation of focal adhesion dynamics and disassembly by phosphorylation of FAK at tyrosine 397, *J. Cell Sci.* 118 (2005) 4415–4425, doi:10.1242/jcs.02565.
- [44] B. da Rocha-Azevedo, F. Grinnell, Fibroblast morphogenesis on 3D collagen matrices: the balance between cell clustering and cell migration, *Exp. Cell Res.* 319 (2013) 2440–2446, doi:10.1016/j.jyexcr.2013.05.003.
- [45] P.L. Ryan, R.A. Foty, J. Kohn, M.S. Steinberg, Tissue spreading on implantable substrates is a competitive outcome of cell-cell vs. cell-substratum adhesivity, *Proc. Natl. Acad. Sci. U.S.A.* 98 (2001) 4323–4327, doi:10.1073/pnas.071615398.
- [46] L.-B. Weiswald, D. Bellet, V. Dangles-Marie, Spherical cancer models in tumor biology, *Neoplasia* 17 (2015) 1–15, doi:10.1016/j.neo.2014.12.004.
- [47] A. Ivascu, M. Kubbies, Diversity of cell-mediated adhesions in breast cancer spheroids, *Int. J. Oncol.* 31 (2007) 1403–1413.
- [48] L. Saias, A. Gomes, M. Cazales, B. Ducommun, V. Lobjois, Cell-cell adhesion and cytoskeleton tension oppose each other in regulating tumor cell aggregation, *Cancer Res.* 75 (2015) 2426–2433, doi:10.1158/0008-5472.CAN-14-3534.
- [49] R.C. Casey, K.M. Burleson, K.M. Skubitz, S.E. Pambuccian, T.R. Oegema Jr., L.E. Ruff, et al., $\beta 1$ -Integrins regulate the formation and adhesion of ovarian

- carcinoma multicellular spheroids, *Am. J. Pathol.* 159 (2001) 2071–2080, doi:10.1016/S0002-9440(10)63058-1.
- [50] Y. Mao, J.E. Schwarzbauer, Fibronectin fibrillogenesis, a cell-mediated matrix assembly process, *Matrix Biol.* 24 (2005) 389–399, doi:10.1016/j.matbio.2005.06.008.
- [51] E. Cukierman, R. Pankov, D.R. Stevens, K.M. Yamada, Taking cell-matrix adhesions to the third dimension, *Science* 294 (2001) 1708–1712, doi:10.1126/science.1064829.
- [52] B.S. Winters, B.M. Raj, E.E. Robinson, R.A. Foty, S.A. Corbett, Three-dimensional culture regulates Raf-1 expression to modulate fibronectin matrix assembly, *Mol. Biol. Cell* 17 (2006) 3386–3396.
- [53] S. Fernandez-Sauze, D. Grall, B. Cseh, E. Van Obberghen-Schilling, Regulation of fibronectin matrix assembly and capillary morphogenesis in endothelial cells by Rho family GTPases, *Exp. Cell Res.* 315 (2009) 2092–2104, doi:10.1016/j.yexcr.2009.03.017.
- [54] C. Zhong, M. Chrzanowska-Wodnicka, J. Brown, A. Shaub, A.M. Belkin, K. Burridge, Rho-mediated contractility exposes a cryptic site in fibronectin and induces fibronectin matrix assembly, *J. Cell Biol.* 141 (1998) 539–551, doi:10.1083/jcb.141.2.539.
- [55] V. Vouret-Craviari, E. Boulter, D. Grall, C. Matthews, E.V. Obberghen-Schilling, ILK is required for the assembly of matrix-forming adhesions and capillary morphogenesis in endothelial cells, *J. Cell Sci.* 117 (2004) 4559–4569, doi:10.1242/jcs.01331.
- [56] D. Ilić, B. Kovačič, K. Johkura, D.D. Schlaepfer, N. Tomašević, Q. Han, et al., FAK promotes organization of fibronectin matrix and fibrillar adhesions, *J. Cell Sci.* 117 (2004) 177–187, doi:10.1242/jcs.00845.
- [57] C.T. Skau, S.V. Plotnikov, A.D. Doyle, C.M. Waterman, Inverted formin 2 in focal adhesions promotes dorsal stress fiber and fibrillar adhesion formation to drive extracellular matrix assembly, *Proc. Natl. Acad. Sci. U.S.A.* 112 (2015) E2447–E2456, doi:10.1073/pnas.1505035112.
- [58] J. Sottile, J. Chandler, Fibronectin matrix turnover occurs through a caveolin-1-dependent process, *Mol. Biol. Cell* 16 (2005) 757–768, doi:10.1091/mbc.E04-08-0672.
- [59] F. Shi, J. Sottile, MT1-MMP regulates the turnover and endocytosis of extracellular matrix fibronectin, *J. Cell Sci.* 124 (2011) 4039–4050, doi:10.1242/jcs.087858.
- [60] T. Takino, R. Nagao, R. Manabe, T. Domoto, K. Sekiguchi, H. Sato, Membrane-type 1 matrix metalloproteinase regulates fibronectin assembly to promote cell motility, *FEBS Lett.* 585 (2011) 3378–3384, doi:10.1016/j.febslet.2011.09.039.
- [61] M.J. Riemenschneider, W. Mueller, R.A. Betensky, G. Mohapatra, D.N. Louis, In situ analysis of integrin and growth factor receptor signaling pathways in human glioblastomas suggests overlapping relationships with focal adhesion kinase activation, *Am. J. Pathol.* 167 (2005) 1379–1387.
- [62] D. Jülich, G. Cobb, A.M. Melo, P. McMillen, A.K. Lawton, S.G.J. Mochrie, et al., Cross-scale integrin regulation organizes ECM and tissue topology, *Dev. Cell* 34 (2015) 33–44, doi:10.1016/j.devcel.2015.05.005.